Measurement of the W-boson helicity in $t\bar{t}$ lepton+jets events

Annik Olbrechts for the CMS Collaboration

Vrije Universiteit Brussel, Pleinlaan 2, 1050 Brussel, Belgium

DOI: http://dx.doi.org/10.3204/DESY-PROC-2014-02/67

The top quark decays almost exclusively to a W-boson and a bottom quark and, due to its high mass, its spin information is passed on to the decay products, restricting the possible decay configurations. The top quark decay is entirely described by the weak charged current, characterized by a V-A structure. Within the Wtb interaction, the right-handed helicity state of the W-boson is suppressed, and at leading order (LO) the longitudinal and left-handed states contribute for 70% and 30%, respectively. These helicity fractions are only slightly influenced by higher-order corrections [1].

Experimentally the W-boson helicity fractions can be obtained by measuring the angular distribution of the W-boson's decay products, for which the dependence is given in Equation 1. The considered helicity angle θ^* is defined as the angle between the direction opposite to the top quark and the direction of the down-type fermion, both boosted to the W-boson rest frame.

$$\frac{1}{\Gamma}\frac{d\Gamma}{d\cos\theta^*} = \frac{3}{8}F_L(1-\cos\theta^*)^2 + \frac{3}{4}F_0(\sin\theta^*)^2 + \frac{3}{8}F_R(1+\cos\theta^*)^2 \quad (1)$$

An accurate measurement of the W-boson helicity fractions is of large importance for the validation of the V-A structure of the weak charged current and for probing physics beyond the Standard Model (SM). Current measurements of the W-boson helicity fractions in top-quark decays [2, 3, 4, 5] are in agreement with the SM predictions. Possible deviations from the SM helicity fractions can be interpreted as anomalous Wtb couplings [6] which are described by the most general dimension-six Lagrangian [7]:

$$\mathcal{L}_{Wtb} = -\frac{g}{\sqrt{2}}\bar{b}\gamma^\mu V_{tb}(V_L P_L + V_R P_R)tW^-_\mu - \frac{g}{\sqrt{2}}\bar{b}\frac{i\sigma^{\mu\nu}q_\nu}{M_W}V_{tb}(g_L P_L + g_R P_R)tW^-_\mu + h.c., \quad (2)$$

where V_L, V_R, g_L, and g_R are complex constants, $q = p_t$ - p_b, where p_t (p_b) is the four-momentum of the top quark (b quark), P_L (P_R) is the left (right) projector operator, and h.c. denotes the Hermitian conjugate. Within the SM V_R, g_L, and g_R are equal to zero, and $V_L = V_{tb} \simeq 1$.

The measurements presented here are based on proton-proton collisions collected by the CMS [8] detector in 2011 at $\sqrt{s} = 7$ TeV, corresponding to an integrated luminosity of 5 fb^{-1}. For this analysis $t\bar{t}$ events for which one of the W-boson decays into a lepton (muon or electron) and corresponding neutrino, and the other one decays into two light jets have been considered. A similar analysis has been performed for data collected in 2012 at 8 TeV, corresponding to 19.6

fb^{-1} integrated luminosity, for which only final states containing a muon have been considered.

The top-quark decay products are reconstructed using the particle-flow algorithm [9]. The events are required to have an isolated lepton, and events with additional muons or electrons are rejected in order to reduce background contributions. The jets are clustered using the anti-k_t algorithm [10] with a distance parameter of 0.5. The full event selection for both the 7 TeV and 8 TeV analysis can be found in Table 1. In the latter analysis additional asymmetric kinematic jet p_T cuts have been applied in order to be consistent with the 8 TeV triggers, requiring the three most energetic jets to have $p_T > 55$, 45, and 30 GeV.

	7 TeV Muon Channel			**7 TeV Electron Channel**			**8 TeV Muon Channel**		
> 4 jets	p_T > 30 GeV	$\|\eta\|$ < 2.4		p_T > 30 GeV	$\|\eta\|$ < 2.4		p_T > 20 GeV	$\|\eta\|$ < 2.5	
Lepton	p_T > 25 GeV	$\|\eta\|$ < 2.1	PFIso < 0.125	E_T > 30 GeV	$\|\eta\|$ < 2.5	PFIso < 0.1	p_T > 26 GeV	$\|\eta\|$ < 2.1	PFIso < 0.12

Table 1: Event selection for the 7 and 8 TeV analysis

In order to reduce the QCD multi-jet background, the transverse mass, M_T, of the leptonically decaying W-boson is required to be greater than 30 GeV. Limiting this M_T variable to 200 GeV reduces the contribution of background events originating from dileptonically decaying $t\bar{t}$ pairs where one lepton escapes detection. In this analysis also a high-efficiency b-tagging algorithm, the Combined Secondary Vertex [11], is required for at least two jets, reducing the QCD background as well as the W-boson production in association with jets (W+jets).

In order to fully reconstruct the top-quark pair topology a kinematic fit [12] is applied which improves significantly the accuracy of the reconstructed $t\bar{t}$ kinematics. In this analysis the use of the $\cos\theta^*$ variable requires the full reconstruction of the kinematics of the neutrino. Since from measurements only the transverse components of this particle are known, the kinematic fit is also used to obtain the z-component of the neutrino. The obtained distributions can be found in Figures 1 and 2 for the 7 and 8 TeV analyses, respectively. For the hadronic branch of the event only the absolute value of $\cos\theta^*_{hadr}$ is considered since the down-type fermion cannot be identified.

The actual determination of the helicity fractions consists of two distinct steps. First a reweighting procedure, based on MC simulation, is used which produces any new helicity $\vec{F}$ starting from the original ones ($F^{SM}_{L,0,R}$) used in the simulation. Each MC semi-leptonic $t\bar{t}$ event is reweighted using the generated $\cos\theta^*$ value, as shown in Equation 3.

$$W(\cos\theta^*_{gen};\vec{F}) = \frac{\frac{3}{8}F_L(1-\cos\theta^*_{gen})^2 + \frac{3}{4}F_0(\sin\theta^*_{gen})^2 + \frac{3}{8}F_R(1+\cos\theta^*_{gen})^2}{\frac{3}{8}F_L^{SM}(1-\cos\theta^*_{gen})^2 + \frac{3}{4}F_0^{SM}(\sin\theta^*_{gen})^2 + \frac{3}{8}F_R^{SM}(1+\cos\theta^*_{gen})^2} \quad (3)$$

Afterwards the helicity fractions are fitted using a binned Poisson likelihood. For each bin of the $\cos\theta^*_{reco}$ distribution the number of expected $N_{MC}(i;\vec{F})$ and observed $N_{data}(i)$ events are compared:

$$\mathcal{L}(\vec{F}) = \prod_{bin\ i} \frac{N_{MC}(i;\vec{F})N_{data}(i)}{N_{data}(i)!} \exp^{-N_{MC}(i;\vec{F})}. \quad (4)$$

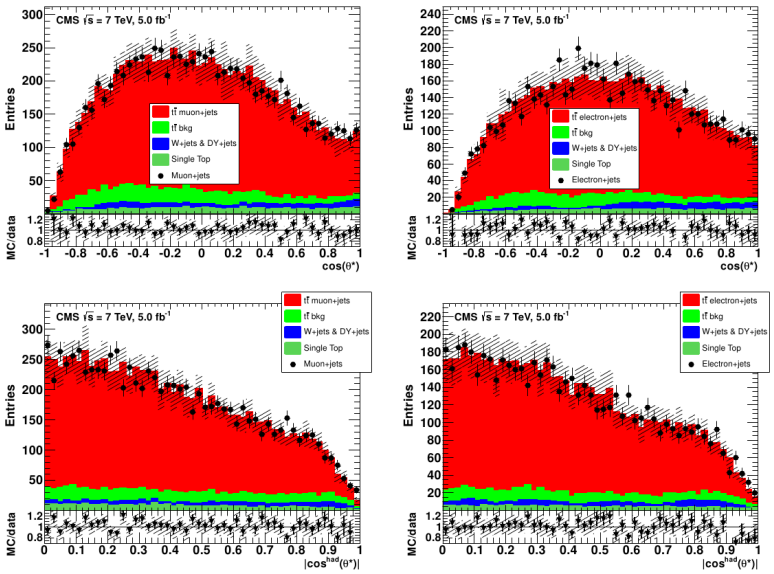

Figure 1: Angular distributions for the muon+jets (left) and electron+jets (right) channels using 7 TeV data. At the bottom, the ratio between prediction and data is given.

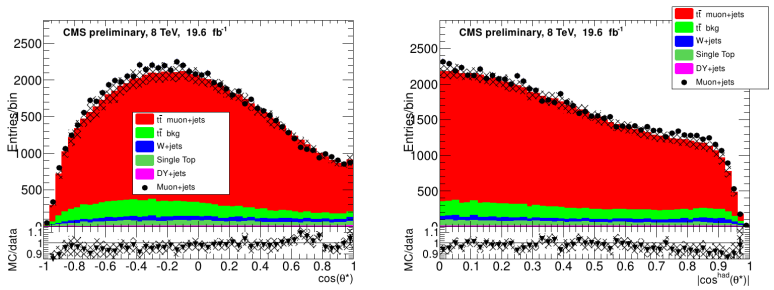

Figure 2: Angular distributions using 8 TeV data. At the bottom, the ratio between prediction and data is given.

The number of expected events are defined in Equations 5-7. For the top-quark pair events an additional normalization component $\mathcal{F}_{t\bar{t}}$ is introduced which absorbs a large fraction of the experimental and theoretical systematics but doesn't influence the helicity fractions.

$$N_{t\bar{t}}(i,\vec{F}) = \mathcal{F}_{t\bar{t}}\left[\sum_{t\bar{t}\ events} W(\cos\theta^*_{gen};\vec{F})\right], \quad (5)$$

$$N_{MC}(i,\vec{F}) = N_{BKG}(i) + N_{t\bar{t}}(i,\vec{F}), \quad (6)$$

$$N_{BKG}(i) = N_{W+jets}(i) + N_{DY+jets}(i) + N_{single-top}(i) + \mathcal{F}_{t\bar{t}} \times N_{t\bar{t}\ non-\ell+jets}(i). \quad (7)$$

In this analysis two different fits are performed. Since the helicity fractions are constrained by unitarity ($F_0 + F_R + F_L = 1$), from Equations 5-7 can be seen that only three parameters

remain free: F_0, F_L, and $\mathcal{F}_{t\bar{t}}$, resulting in the so-called 3D fit. In case of the 2D fit the number of free parameters is further reduced by constraining the right-handed helicity fraction to the SM prediction ($F_R = 0$).

Several sources of systematic uncertainties are investigated and listed in Table 2. The simulated backgrounds have been scaled with a percentage of ±15%, ±40%, ±30%, and ±100%, respectively for the single-top t-channel, single-top tW channel, DY+jets sample, and W+jets sample to obtain their influence on the measurement of the helicity fractions. As can be seen from the table, the dominant sources of background for the 7 TeV analysis are the W+jets background normalization, the signal modelling, and the statistics of the simulated samples. The hadronic branch, using $|\cos^{had}\theta^*|$, has significant larger systematic uncertainties mainly due to the dominant W+jets background and the contribution of JES, JER, and PDF uncertainties, and are not shown in the Table.

For the 8 TeV analysis the dominant backgrounds are rather similar, with the additional studied E_T^{miss} distribution being very important. For this dataset, it was observed that the slope of the E_T^{miss} distribution obtained in data was not well reproduced in simulation. Therefore a reweighting was done for the simulated events and the difference in obtained helicity fractions was taken as systematic.

	7 TeV systematics			8 TeV systematics	
	3D fit		2D fit	3D fit	
	$\pm\ \Delta\ F_0$	$\pm\ \Delta\ F_0$	$\pm\ \Delta\ F_0$	$\pm\ \Delta\ F_0$	$\pm\ \Delta\ F_0$
JES	0.006	0.003	0.001	0.002	< 0.001
JER	0.011	0.007	0.001	0.004	0.003
Lepton eff.	0.001	0.002	0.002	0.001	< 0.001
b-tag eff.	0.001	$< 10^{-3}$	$< 10^{-3}$	0.001	< 0.001
Pileup	0.002	$< 10^{-3}$	0.008	< 0.001	0.001
Single-t bkg.	0.004	0.001	0.003	0.002	< 0.001
W+jets bkg.	0.013	0.004	0.006	0.001	< 0.001
DY+jets bkg.	0.001	$< 10^{-3}$	0.001	0.009	< 0.001
MC statistics	0.016	0.012	0.010	0.003	0.002
Top-quark mass	0.016	0.011	0.019	0.012	0.008
$t\bar{t}$ scales	0.009	0.009	0.011	0.012	0.012
$t\bar{t}$ match. scale	0.011	0.010	0.008	0.012	0.008
PDF	0.002	$< 10^{-3}$	0.003		
$t\bar{t}$ p_T reweig.				0.001	< 0.001
E_T^{miss} shape				0.004	0.018

Table 2: Systematics for the combined lepton+jets channel for both the 3D and 2D fit obtained from fitting the leptonic branch of the event.

For the 7 TeV analysis the most precise measurement was obtained using a 3D fit on the leptonic branch of the event. The results combining the muon and electron channel are:

$$\begin{cases} F_0 = 0.682 \pm 0.030\ (\text{stat}) \pm 0.033\ (\text{syst}), \\ F_L = 0.310 \pm 0.022\ (\text{stat}) \pm 0.022\ (\text{syst}), \\ F_R = 0.008 \pm 0.012\ (\text{stat}) \pm 0.014\ (\text{syst}). \end{cases}$$

These measured helicity fractions have been used to set limits on the anomalous couplings. For this two specific scenarios have been considered for both of which CP conservation is assumed. For the first scenario $V_L = 1$, $V_R = g_L = 0$ are set and $\text{Re}(g_R)$ is considered as a

free parameter. The result is shown in Equation 8 and can be translated in terms of effective operators [6], given in Equation 9. Secondly $\mathrm{Re}(g_L)$ and $\mathrm{Re}(g_R)$ are chosen as free parameters of the fit. Figure 3 shows the regions of the $\mathrm{Re}(g_L)$, $\mathrm{Re}(g_R)$ plane allowed at 68% and 95% CL.

$$\mathrm{Re}(g_R) = -0.008 \pm 0.024\ (\mathrm{stat})^{+0.029}_{-0.030}\ (\mathrm{syst}) \quad (8)$$

$$\frac{1}{\Lambda^2}\mathrm{Re}(C^{33}_{uW}) = -0.088 \pm 0.280\ (\mathrm{stat})^{+0.339}_{-0.352}\ (\mathrm{syst})\ \ \mathrm{TeV}^{-2} \quad (9)$$

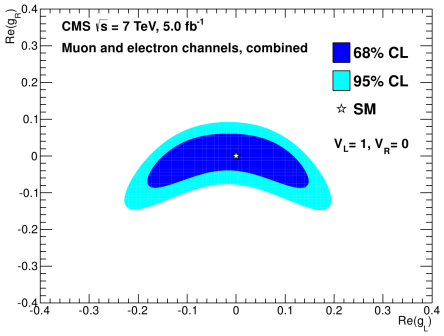

Figure 3: Regions of the $\mathrm{Re}(g_L)$, $\mathrm{Re}(g_R)$ plane allowed at 68% and 95% CL

For the 8 TeV analysis the measurement was only performed using a 3D fit on the leptonic branch of the event, for which the helicity fractions yield:

$$\begin{cases} F_0 = & 0.659 \pm 0.015\ (\mathrm{stat}) \pm 0.023\ (\mathrm{syst}), \\ F_L = & 0.350 \pm 0.010\ (\mathrm{stat}) \pm 0.024\ (\mathrm{syst}), \\ F_R = & -0.009 \pm 0.006\ (\mathrm{stat}) \pm 0.020\ (\mathrm{syst}). \end{cases}$$

References

[1] A. Czarnecki, J. G. Korner and J. H. Piclum, Phys. Rev. D **81** (2010) 111503, arXiv:1005.2625 [hep-ph].

[2] T. Aaltonen *et al.* [CDF and D0 Collaborations], Phys. Rev. D **85** (2012) 071106, arXiv:1202.5272 [hep-ex].

[3] G. Aad *et al.* [ATLAS Collaboration], JHEP **1206** (2012) 088, arXiv:1205.2484 [hep-ex].

[4] S. Chatrchyan *et al.* [CMS Collaboration], JHEP **1310** (2013) 167, arXiv:1308.3879 [hep-ex].

[5] CMS Collaboration, CMS-PAS-TOP-13-008.

[6] J. A. Aguilar-Saavedra, Nucl. Phys. B **812** (2009) 181, arXiv:0811.3842 [hep-ph].

[7] J. A. Aguilar-Saavedra and J. Bernabeu, Nucl. Phys. B **840** (2010) 349, arXiv:1005.5382 [hep-ph].

[8] S. Chatrchyan *et al.* [CMS Collaboration], JINST **3** (2008) S08004.

[9] CMS Collaboration, CMS-PAS-PFT-10-002.

[10] M. Cacciari, G. P. Salam and G. Soyez, JHEP **0804** (2008) 063, arXiv:0802.1189 [hep-ph].

[11] S. Chatrchyan *et al.* [CMS Collaboration], JINST **8** (2013) P04013, arXiv:1211.4462 [hep-ex].

[12] J. D'Hondt, S. Lowette, O. L. Buchmuller, S. Cucciarelli, F. P. Schilling, M. Spiropulu, S. Paktinat Mehdiabadi and D. Benedetti *et al.*, CERN-CMS-NOTE-2006-023.